Journal of Natural Fibers

ISSN: (Print) (Online) Journal homepage: https://www.tandfonline.com/loi/wjnf20

Effect of ultrafine grinding and ultrasonication duration on the performance of polyvinyl alcohol (PVA) agave gigantea cellulose micro fiber (CMF) bio-composite film

Edi Syafri, Jamaluddin Jamaluddin, Nasmi Herlina Sari, Melbi Mahardika, Lisman Suryanegara, Rafles Sinaga, Ferriawan Yudhanto, Rahadian Zainul, Agus Nugroho, Anish Khan & Mohammad A. Wazzan

To cite this article: Edi Syafri, Jamaluddin Jamaluddin, Nasmi Herlina Sari, Melbi Mahardika, Lisman Suryanegara, Rafles Sinaga, Ferriawan Yudhanto, Rahadian Zainul, Agus Nugroho, Anish Khan & Mohammad A. Wazzan (2023) Effect of ultrafine grinding and ultrasonication duration on the performance of polyvinyl alcohol (PVA) agave gigantea cellulose micro fiber (CMF) bio-composite film, Journal of Natural Fibers, 20:1, 2192545, DOI: 10.1080/15440478.2023.2192545

To link to this article: https://doi.org/10.1080/15440478.2023.2192545

Published online: 24 Mar 2023.

JOURNAL OF NATURAL FIBERS
2023, VOL. 20, NO. 1, 2192545
https://doi.org/10.1080/15440478.2023.2192545

Effect of ultrafine grinding and ultrasonication duration on the performance of polyvinyl alcohol (PVA) agave gigantea cellulose micro fiber (CMF) bio-composite film

Edi Syafri[a,b], Jamaluddin Jamaluddin[a], Nasmi Herlina Sari[c], Melbi Mahardika[b,d], Lisman Suryanegara[b,d], Rafles Sinaga[d], Ferriawan Yudhanto[e], Rahadian Zainul[f], Agus Nugroho[g], Anish Khan[h], and Mohammad A. Wazzan[i]

[a]Department of Agricultural Technology, Politeknik Pertanian Negeri Payakumbuh, West Sumatra, Indonesia; [b]Research Collaboration Center for Nanocellulose, BRIN and Andalas University, Padang, Indonesia; [c]Department of Mechanical Engineering, Faculty of Engineering, University of Mataram, Mataram, Indonesia; [d]Research Center for Biomass and Bioproducts, National Research and Innovation Agency of Indonesia (BRIN), Cibinong, Indonesia; [e]Department of Mechanical Technology, Universitas Muhammadiyah Yogyakarta, Yogyakarta, Indonesia; [f]Department of Chemistry, Faculty of Mathematics and Natural Sciences, Universitas Negeri Padang, Padang, Indonesia; [g]Faculty of Mechanical and Automotive Engineering Technology, Universiti Malaysia Pahang, Kuantan, Pahang, Malaysia; [h]Center of Excellence for Advanced Materials Research, King Abdulaziz University, Jeddah, Saudi Arabia; [i]Department of Radiology, King Abdulaziz University, Jeddah, Saudi Arabia

ABSTRACT

This paper aims to assess the effect of ultrafine grinding and ultrasonication treatment on the bio-composite characteristics of polyvinyl alcohol (PVA) Agave gigantea (AG) Cellulose Micro Fiber (CMF) bio-composite film performance. This study included five different types of samples. FESEM investigation of PVA/CMF revealed a fiber diameter of 10–15 µm. According to X-ray diffraction, the CMF bio-composite has the highest crystallinity index (87%). The bio-composite film was as transparent as the pure PVA film, demonstrating that the CMF was uniformly dispersed throughout the film. Tensile testing revealed that the ultrafine grinding and ultrasonication treatment for 2 h (PVA/U2) increased tensile strength by 43% compared to the untreated PVA/CMF sample. This finding is confirmed by thermogravimetry analysis (TGA) and derivative (DTG) analyses, which show that the PVA/U2 sample has the most significant degree of thermal stability when compared to other samples. An ANOVA output supports the results of this experiment with an R2 value of 0.94600232 at a 95% confidence level. The p-value of 0.000079 and F-value of 10.80004 for ultrafine grinding and ultrasonication duration on AG leaf-based PVA bio-composite revealed a statistically significant influence on the studied parameters.

摘要

本文旨在评估超细研磨和超声处理对聚乙烯醇（PVA）龙舌兰（AG）纤维素微纤维（CMF）生物复合膜性能的影响. 这项研究包括五种不同类型的样本。PVA/CMF的FESEM研究显示纤维直径为10-15 µm. 根据X射线衍射, CMF生物复合材料具有最高的结晶度指数（87%）. 生物复合膜与纯PVA膜一样透明, 表明CMF均匀分散在整个膜中. 拉伸测试表明, 与未处理的PVA/CMF样品相比, 超细研磨和超声处理2小时（PVA/U2）使拉伸强度提高了43%. 热重分析（TGA）和导数（DTG）分析证实了这一发现, 表明与其他样品相比, PVA/U2样品具有最显著的热稳定性. 方差分析输出在95%置信水

KEYWORDS

Agave gigantea; cellulose microfiber; ANOVA, superior thermal stability and high transparency

关键词

龙舌兰; 纤维素微纤维; 优异的热稳定性和高透明度

CONTACT Melbi Mahardika melbi.mahardika@brin.go.id Research Center for Biomass and Bioproducts, National Research and Innovation Agency of Indonesia (BRIN), Cibinong 16911, Indonesia

This article has been republished with a minor change. This change does not impact on the academic content of the article.

平下支持该实验的结果, R2值为0.94600232. AG叶基PVA生物复合材料的超细研磨和超声持续时间的p值为0.000079, F值为10.80004, 显示出对所研究参数的统计学显著影响.

Introduction

Polyethylene (PE) (Mohammadi and Babaei 2022; Moradi et al. 2020), polypropylene (PP) (Akoueson et al. 2023; da Silva et al. 2022), polystyrene (PS) (Abolghasemi-Fakhri et al. 2019; Pilevar et al. 2019), polyvinyl chloride (PVC) (Chen et al. 2022 H. Wang et al. 2022), and polyethylene terephthalate (PET) (Yuan et al. 2023; Zhai et al. 2022) are now the most common raw materials employed in the manufacture of traditional plastics for packaging applications. However, because they are non-biodegradable, these plastics generate severe worldwide environmental issues (Haider et al. 2019; Taghavi et al. 2021). Therefore, biodegradable polymers are used to replace the plastics material due to its environmentally friendly, abundant availability, and sustainable. Among biodegradable polymers, Polyvinyl Alcohol (PVA) has superior properties: biocompatible, semi-crystalline, nontoxic, water-soluble, chemical resistant, transparency, great flexibility, and outstanding physical properties (Allafchian et al. 2020; Cano et al. 2015; Dara et al. 2021; Poyraz et al. 2017). PVA can form hydrogen bonds with the surface of hydrophilic materials and serves as a matrix for bio-composite material (Lisdayana et al. 2020; Sarwar et al. 2018).

However, PVA films have poor mechanical and thermal properties, which could limit their utility in packaging applications (Cazón, Vázquez, and Velazquez 2018a, 2018b; Huang et al. 2019). There are several investigations on cellulose-reinforced PVA matrix to increase the tensile strength and thermal stability of PVA composite (Hu and Wang 2016; Singh, Gaikwad, and Suk Lee 2018; Wu et al. 2022). Cellulose fibers are widely used as polymer reinforcement because they are renewable, sustainable, abundant, and low-cost. Notably, cellulose has outstanding mechanical characteristics such as high tensile strength and elastic moduli owing to its semi-crystalline extended polymer chain (Candan et al. 2022; Poyraz et al. 2018; Tozluoglu et al. 2022). Cellulose provides a larger reaction surface with the matrix because of the presence of hydrogen bonds, resulting in a better and promising strengthening effect in bio-composite production (Kalambettu et al. 2015). The cellulose structure can be deconstructed through chemical and mechanical treatments to reduce cellulose fibrefibres' size from raw cellulose microfibers (CMF). CMF can be extracted from numerous sources, including leaves or stiff fibers, wood, cereal straws, seeds, fruits, bamboo fiber, sugar palm fiber, ginger, agave, and other plant fibers. Among them, Agave gigantea showed a cellulosic fiber content of around 55–70%, higher than wood, with values ranging from 40% to 50% (Azammi et al. 2020 S. K. Singh et al. 2021). In this work, various sizes of CMF from agave fibers through chemical treatment (alkalization and lightening), ultrafine crushing, and ultrasonication have been developed.

Furthermore, the CMF was used as reinforcement in PVA-based bio-composites, and its mechanical, thermal, transparency and functional groups were examined. FESEM was used to examine the fracture surface of composites and the shape and diameter of agave fibers from various treatments. This paper elaborates on how ultrafine grinding and ultrasonic treatment affect the mechanical and thermal properties of PVA films Agave gigantea bio-composite. Although there have been many previous studies reporting on the improvement of properties of bio-composite films, relatively limited information has been available regarding the effect of Agave gigantea content on several properties that are important in food packaging applications; mechanical properties, thermal stability, and film transparency characterization of PVA-based bio-composites. Properties measured were transparency, thermal stability (using differential scanning calorimetry (DSC) and thermogravimetric analysis (TGA)), and tensile properties. All samples were also characterized by field emission scanning electron microscopy (FESEM), and x-ray diffraction (XRD).

Materials and methods

Materials

The fiber in this work was extracted from the fresh leaves of the Agave gigantea (AG) plant. The leaves were sourced in the plantation area in Harau District, West Sumatera Indonesia. Polyvinyl alcohol with 99% hydrolyzed was supplied from Sigma-Aldrich, United States of America. The chemicals adopted in this experiment were sodium hydroxide (NaOH), sodium chlorite ($NaClO_2$), and glacial acetic acid (CH_3COOH).

Sample preparation

Fresh AG leaves were cleansed and sliced into 100–120 mm lengths before being immersed in boiling water at 100°C for 3 h to enhance fiber release from other extractive elements. The outer skin of the fiber was then removed with a stainless cutter. The AG fiber was sun-dried for 3–4 days with a moisture level of 9% to 11%. The AG fiber was sliced into 7–12 mm lengths and mashed with a blender. On a hotplate, the fibre was alkalized with 5% (w/v) NaOH for 2 h at 80°C. The bleaching was continued using NaClO2 with the condition 1.7% (wt% NaClO2), and then the sample after chemical treatment was labeled CMF. CMF pulp with a suspension concentration of 1 wt% and a dry weight of 20 g of cellulose was suspended in 2000 mL of distilled water with a modified previous study (Syafri et al. 2021, 2021). The solution was fed into the Masuko Sangyo ultrafine grinder MKCA6–3; Masuko Sangyo Co., Ltd., Japan, with various gaps of −10, −30, −50, −70, −90, and −110 m to obtain CMF, with five passes each in each gap. The resulting CMF suspension showed the characteristics of a gel labeled UFG AG. Furthermore, this cellulose suspension was ultrasonicated using SONIC RUPTOR 400 Omni International for 1 h and 2 h at 600 W with the labels U1 and U2 AG. The CMF formulation process is shown in the schematic diagram in Figure 1.

There are five samples in this study, namely PVA film (100 mL of distilled water and 10 g of PVA), PVA/CMF AG film (100 mL of distilled water, 10 g of PVA, and 5 wt% of CMF), PVA/UFG AG film (100 mL of distilled water, 10 g of PVA, and 5 wt% of UFG), PVA/U1 AG film (100 mL of distilled water, 10 g of PVA, and 5 wt% of pure UI) subjected with ultrasonication for 1 h, and PVA/U1 AG film (100 mL of distilled water, 10 g of PVA, and 5 wt% of pure UI) subjected with ultrasonication for two h. A magnetic stirrer was used to mix the components to form a fiber suspension. Meanwhile, ultrasonication treatment was done to the samples to improve the sample components' dispersion in the suspension (Abral et al. 2019; Mahardika et al. 2019).

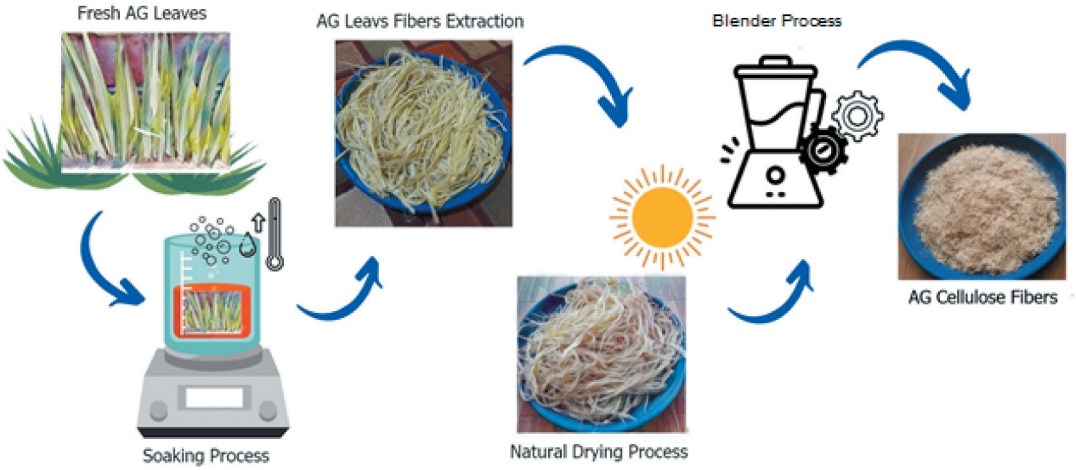

Figure 1. Schematic diagram of sample preparation.

One hundred milliliters of Distilled water and 10 g of PVA were mixed to prepare PVA film. The suspension was heated at 70°C and 500 rpm for 2 h until gelatinized using the magnetic stirrer Scilogex MS-H280-Pro. The resulting gel was sonicated by SONIC RUPTOR 400 Omni International ultrasonic for 5 min. The treated gel cast in a beaker was dried for 20 h in a 50°C vacuum drying oven at 0.6 MPa.

5 wt% of CMF and 10 g of PVA were dispersed into 100 mL of distilled water PVA/CMF AG film. The suspension was heated using a magnetic stirrer at 70°C and 500 rpm for 2 h until gelatinization. The resulting gel was treated with 600 W for 5 min using the ultrasonic SONIC RUPTOR 400 Omni International. The treated gel cast in a beaker was dried for 20 h in a 50°C vacuum drying oven at 0.6 MPa.

Five percent of pure UFG AG suspension, 10 g of PVA, and 10 mL of distilled water were heated on the magnetic stirrer at 70°C and 500 rpm for 2 h until gelatinization to form PVA/UFG AG film. The resulting gel was treated with 600 W ultrasonic for 5 min. The treated gel cast in a beaker was dried for 20 h in a 50°C vacuum drying oven at 0.6 MPa.

The suspension (10 g PVA, 5% pure UI, and 100 mL distilled water) was heated by the magnetic stirrer at 70°C and 500 rpm for 2 h until gelatinization to form PVA/U1 AG film. The resulting gel was sonicated at 600 W for 5 min. The sonicated gel was cast in a beaker and dried for 20 h in a 50°C vacuum drying oven at 0.6 MPa as suggested in the previous study (Syafri et al. 2021).

PVA/U2 AG film was prepared by mixing 10 g of PVA, 10 g PVA, 5% pure UI, and 100 mL of distilled water pure UI in the suspension (10 g PVA, 5% pure UI, and 100 mL distilled water) was heated by the magnetic stirrer at 70°C and 500 rpm for 2 h until gelatinization. The resulting gel was sonicated at 600 W for 5 min. The sonicated gel was cast in a beaker and dried for 20 h in a 50°C vacuum drying oven at 0.6 MPa. All films were stored in a closed desiccator device at 50% relative humidity and 25 C before sample characterization (Yun et al. 2022).

Field emission scanning electron microscopy characterization

A field emission scanning electron microscope (FESEM) Quattro S, Thermo Fisher Scientific, Waltham, MA, USA, was employed to assess the morphological fracture surfaces of the films. As suggested by previous researchers, the sample was placed in the carbon tube due to the non-conductive sample type (Nugroho et al. 2021; Taspika et al. 2020). The FESEM images of the film were recorded at 500 and 2000 magnifications under a high vacuum and working distance of 10 ± 0.5 mm with 3.0 kV accelerating voltage as suggested by previous researchers (Doustdar, Olad, and Ghorbani 2022; Kashyap et al. 2022).

Film transparency characterization

A Shimadzu UV 1800 spectrophotometer was employed to measure the transparency of films according to ASTM D 1003–00 (ASTM 2006). An equal-weight rectangular sample (10 mm × 25 mm) was positioned in the spectrophotometer by a transmittance spectrum of 200 to 800 nm. The transparency of the film is based on the area under the transmittance curve as recommended by previous researchers (da Silva et al. 2022).

Tensile stress assessment

Tensile strength was adopted according to the ASTM D638-type V standard (ASTM 2012). The width and thickness of the samples were measured with 0.01 μm accuracy with digital callipers Mitutuyo Universal Testing Machine AGS-X series 5 kN, Shimadzu, Japan, was employed to govern tensile strength (TS), elastic modulus (ME), and strain at break (SB) of the samples at room temperature. A 30 mm/min tensile test speed was used. Previous researchers (Ding, Tang, and Zhu 2022; Han, Jiang,

and Jinlian 2020) suggested that the tensile tests were repeated five times for each sample to ensure the consistency and reliability of the data (Joshi and Patel 2022; Poyraz et al. 2017).

X-Ray diffraction assessment

Shimadzu XRD-700 Maxima X series from Shimadzu Corp., Kyoto, Japan, was employed to conduct X-ray diffraction testing at 24°C, 40 kV, and 30 mA using Cu Kα radiation (λ = 0.15406 nm) (C. Wang et al. 2020). All samples were scanned from 2θ = 10° to 50° every 2°/min. The Gaussian function was used for the crystallinity calculation (Xc) of the area of the crystalline region and the area of the amorphous region, respectively. Eq. 1 was adopted to calculate the degree of crystallinity:

$$X_c(\%) = (F_c/F_a + F_c)x100 \quad (1)$$

F_c is the crystalline area (2θ = 20–23°), and F_a is the non-crystalline/amorphous region (2θ = 15–16 °).

Thermogravimetry analysis (TGA) and derivative (DTG) assessment

The samples in this work were analyzed using a TGA 4000 thermal analysis instrument from Perkin Elmer, Hopkinton, MA, United States of America. Ten milligrams of the film was placed on a microbalance inside the furnace. The instrument had a nitrogen flow rate of 20 mL/min. The test was carried out from 30°C up to 600°C. Pyris software (Version 11, Pyris, Washington, MA, USA) assessed weight loss, weight loss rate, and residue percentages (Candan, Gardner, and Shaler 2016).

Differential Scanning Calorimetry (DSC)

DSC analysis of the samples was performed using differential scanning calorimetry (DSC) type PerkinElmer 4000, United States. The samples were encapsulated in an aluminum pan then scanned from 30°C to 400°C with a heating rate of 10°C/min under nitrogen gas (Sultana et al. 2020).

Statistical analysis

The variance analysis (ANOVA) was employed to evaluate the tensile property data of films. The difference between samples was determined to be significant at alpha 0.05 with a 95% confidence level.

Results and discussion

Field emission scanning electron microscopy analysis

Figure 2 shows the fracture surface of the PVA/CMF AG bio-composite and the AG fiber's surface morphology after alkalization, bleaching, and ultrasonication for 1 and 2 h. Figure 2(f) shows the surface morphology of cellulose with a magnification of 8000× shows fiber measurements with an average fiber diameter of 8 μm. The presence of non-cellulose material causes a rough surface. Figure 2 (g) shows the surface morphology of the bundled microfibrils. Because of the applied chemical treatment, the fiber diameter was lower (10–15 μm) than the raw AG fiber. Figure 2(d) depicts the smooth surface structure of the fibers in various sizes. Mechanical ultrafine grinding treatment promoted the cellulose to shrink and form micro-dimensional fibers, also known as cellulose micro-fibers.

Figure 2(a) shows a smooth fracture surface of pure PVA due to crack propagation in the presence of resistance. The addition of MCF presence of the surface rougher, as shown in Figure 2(b), because the fibers inhibited crack propagation (Jain, Kumar Singh, and Chauhan 2017; Solikhin et al. 2018). Figure 2(c) shows that the fiber surface is still micro-sized in the PVA matrix. A beach mark due to

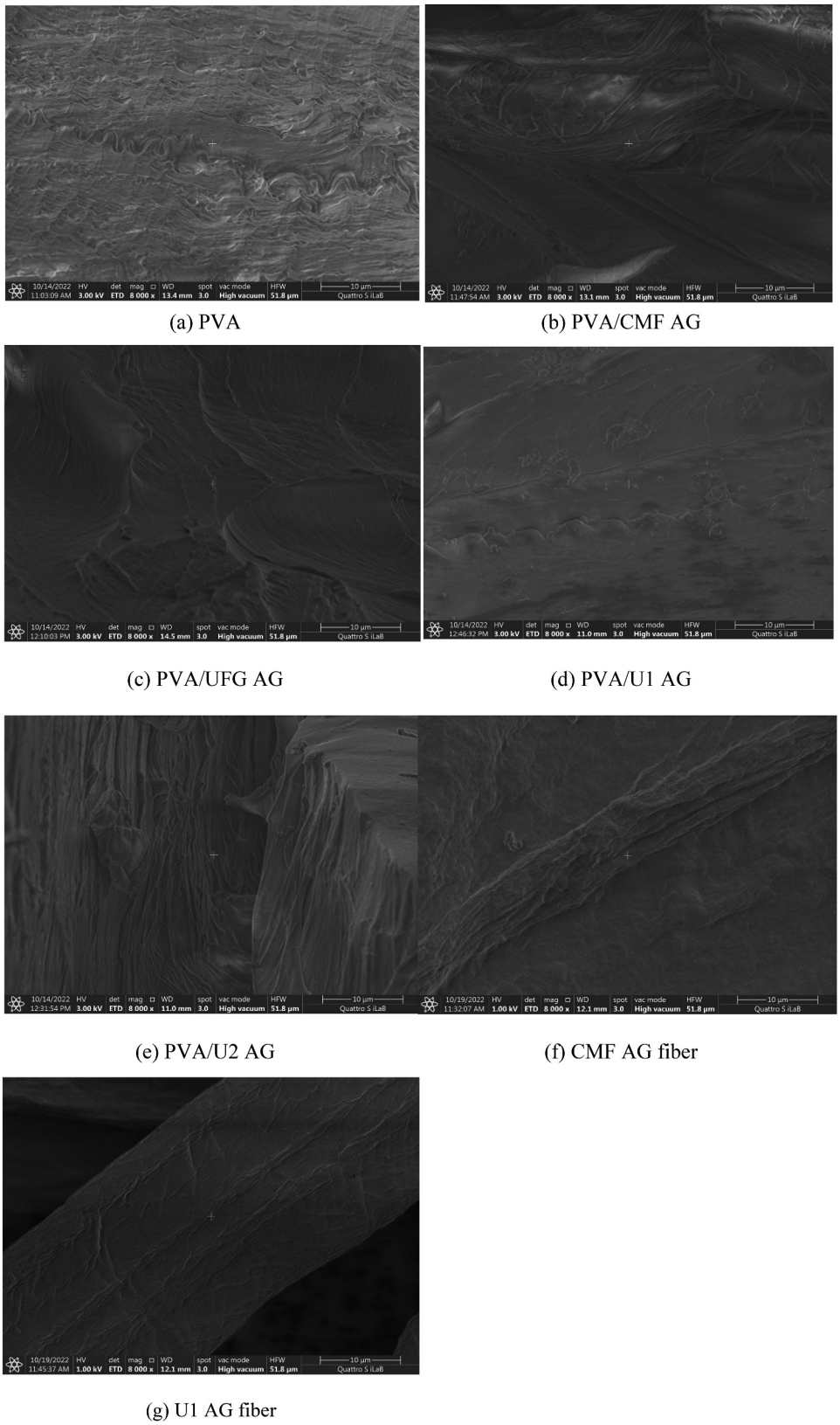

Figure 2. (a-e) FESEM images of the fracture surface PVA and bio-composite PVA/CMF; and (e, f) Morphology of CMF and U1 AG fiber.

cellulose micro-fiber interfering with crack growth is shown in Figure 2(d). The fracture surface of the bio-composite film shows uniformly distributed beach marks over the entire surface, indicating good CMF dispersion after ultrasonication, as shown in Figure 2(e). Besides, the porosities are not visible in Figure 2(e). This event can be explained by the fact that all extracted CMF are well dispersed in the suspension.

Film transparency assessment analysis

The transmittance of PVA and PVA/AG fibers' optical properties were determined in the range of 200–800 nm as shown in various sizes as shown in Figure 3. Film transparency, % transmittance at 280 and 660 nm, and UV block for PVA films with different sizes of AG fiber were analyzed (Table 1). % T film predominantly depends on the dispersion of the AG fiber in the PVA matrix. The PVA film became relatively opaque with the AG fiber content after UFG, decreasing from 76% T for pure PVA to 65% T. The UFG cellulose suspension reduced the light transmittance of the PVA bio-composite films concerning the higher cellulose content revealing better dispersion in the matrix. PVA films with a mixture of CMF, U1, and U2 AG fibers exhibited high transparency of about 90%, 87%, and 89%, respectively. Another advantage of this film is its high UV absorption capacity, blocking 61%, 52%, and 47% of UV-B, respectively. UFG causes a decrease in the transparency of the film. It significantly lowers the UV absorption capacity. For the chemical composition of cellulose, the smaller the size of the cellulose leads to a more significant increase in UV absorption. These results are supported by previous research (Feiya et al. 2015)(Q. Wang et al. 2018).

Tensile stress properties analysis

Figure 4 depicts the mechanical properties of the tensile strength (TS), elastic modulus (ME), and strain at break (SB) of PVA films and PVA bio-composites with the addition of cellulose AG fibers of different sizes. The cellulose microfiber AG in the PVA matrix observed a significant decrease in

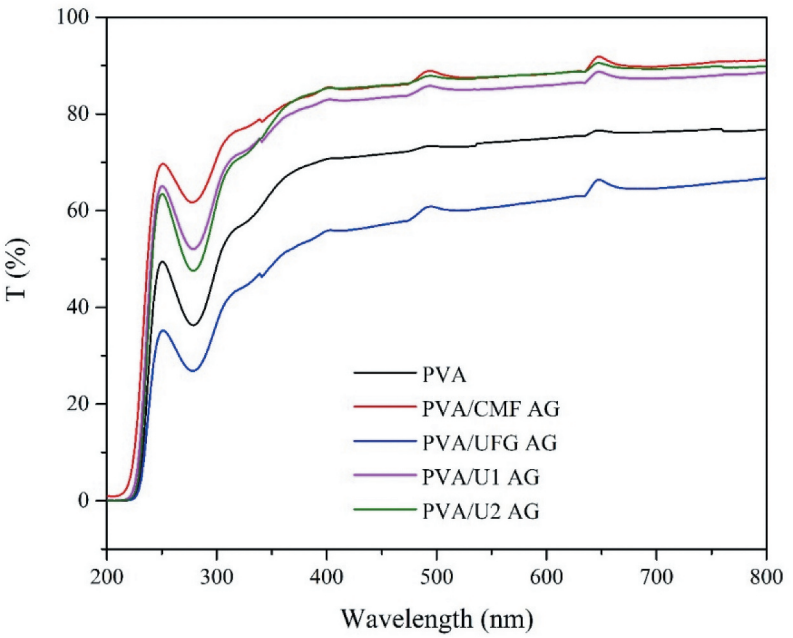

Figure 3. Transmittance versus wavelength of all samples.

Table 1. Crystallinity index, %T at 280 and 660 nm, and Tmax of PVA and bio-composite PVA.

Sample	CI (%)	%T at 280 nm	%T at 660 nm	T_{max} (°C)
PVA	85.8	36	76	333.3
PVA/CMF AG	87.0	61	90	334.8
PVA/UFG AG	83.0	26	65	335.7
PVA/U1 AG	85.6	52	87	336.4
PVA/U2 AG	84.9	47	89	341.6

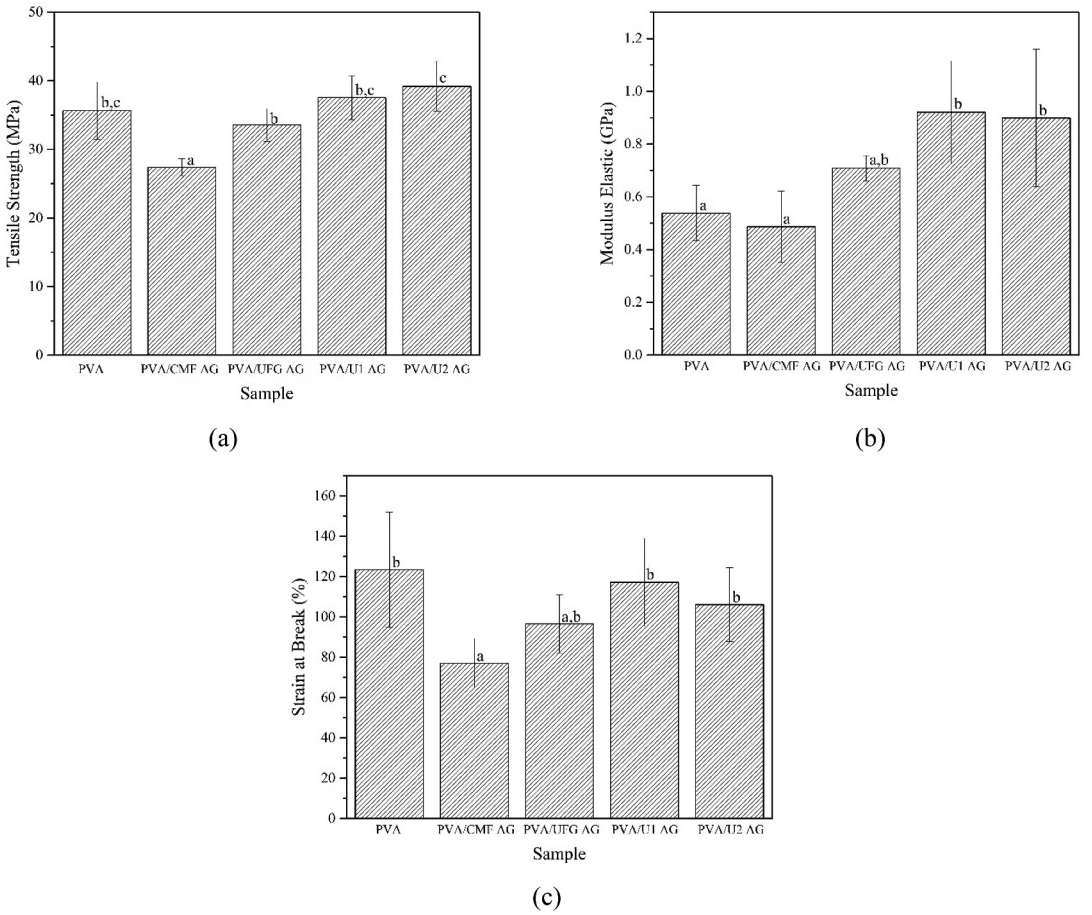

Figure 4. Tensile properties as a function of AG fiber for (a) Tensile Strength, (b) Modulus Elastic, and (c) Strain at the break.

tensile strength. A significant increase was observed using UFG, U1, and U2 AG fibers (33 MPa, 37 MPa, and 39 MPa, respectively). A similar trend has resulted when analyzing the elastic modulus of the films. These measures of tensile strength are a great deal higher than those measured in PVA and ginger nanofiber (Abral et al. 2020). Abral et al. (2020) reported the tensile strength of PVA films with 7.5 mL nanofiber were 37.5 MPa, respectively.

After ultrafine grinding and ultrasonication, the addition of cellulose AG fiber improved the mechanical properties of PVA films. This improvement was attributed to three factors: (i) inherent chain stiffness; (ii) homogeneous distribution of cellulose AG fiber in the PVA matrix; and (iii) high

compatibility between cellulose AG fiber and PVA, resulting in a strong interaction through hydrogen bonding. Although introducing various cellulose AG fiber diameters provided a comparable result, not all of them strengthened the PVA matrix similarly. The PVA film's tensile strength was calculated to be 27.40 MPa. It did not increase significantly with the addition of UFG to 33.55 MPa. However, after adding U2 AG, the tensile strength increased by 17% (39.20 MPa).

In contrast, the elastic modulus increased with the addition of UFG, U1, and U2 by increasing the values of 708.64 MPa, 921.08 MPa, and 898.83 MPa, respectively, compared to pure PVA (538.21 MPa). Variations in the cellulose AG fibre size can explain the difference in the strengthening effect of cellulose macro-fiber. The ultrafine grinding and ultrasonication process promoted the micro-cellulose's surface area enhancement. This event escalated the pure PVA film's cellulose microfibers' tensile properties (Abdulkhani, Echresh, and Allahdadi 2020; Li et al. 2022). The cellulose AG fibre's size can affect the PVA matrix's strengthening effect. Previous studies (Anwer et al. 2015; Kumar, Kumar, and Bhowmik 2018) reported that cellulose micro-fiber produces a higher specific surface area which causes cross-linking, contributing to an increase in tensile properties. In addition, during the mechanical treatment, the strain at break increased due to the cellulose micro-fiber content. This phenomenon can be attributed to the between and within the molecular hydrogen bonding of cellulose micro-fiber with PVA increasing its elasticity and tensile properties. These results are supported by previous research (Nurazzi et al. 2021).

X-Ray diffraction assessment analysis

The XRD patterns of all the formulated samples are compared in Figure 5 with different sizes of cellulose, namely PVA/CMF AG, PVA/UFG AG, PVA/U1 AG, and PVA/U2 AG. The PVA film's crystallinity and bio-composite were computed using the Segal method. PVA and bio-composite PVA peaks at a value of 2θ from 20°.

However, the prominent peak of PVA was observed at 19.5, representing the (11O) plane of the partially semi-crystalline region of PVA Jahan, Bilal Khan Niazi, and Weiby Gregersen (2018); Niazi et

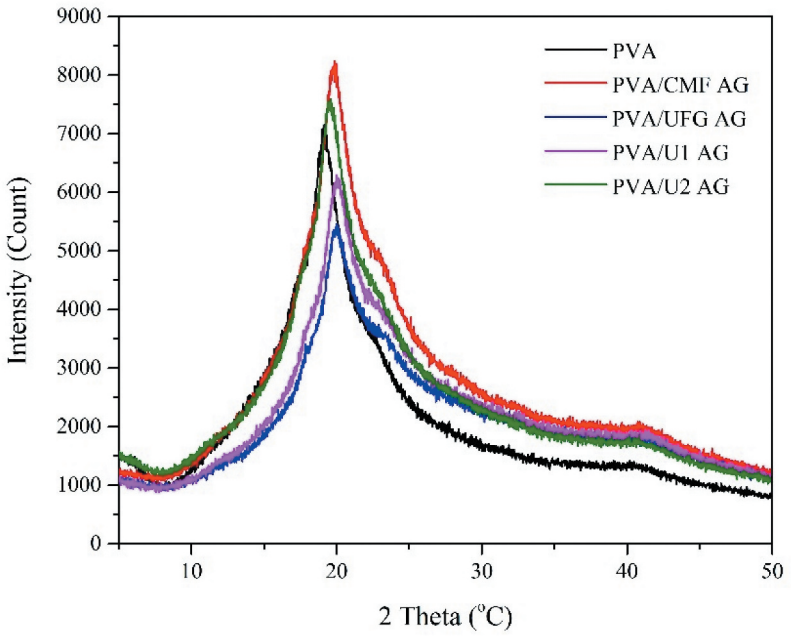

Figure 5. The XRD patterns of all samples.

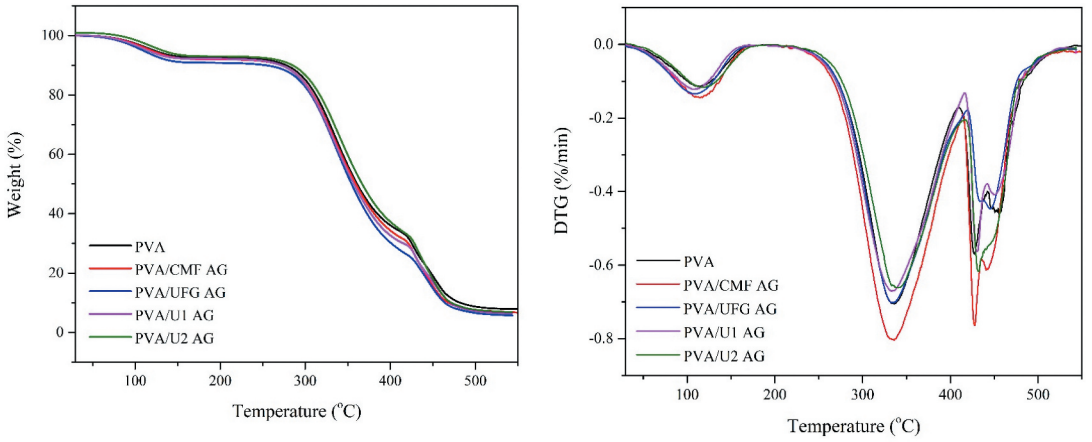

(a) TGA result of various samples (b) DTG result of various samples

Figure 6. (a) TGA and b) DTG of PVA and (b) PVA/MCF AG fiber bio-composite.

al. (2017). In PVA films, the crystallinity was slightly lower than that of PVA/CMF AG. The addition of cellulose microfiber AG into the PVA bio-composite film increased the intensity (11O), increasing crystallinity. PVA/CMF AG had the highest crystallinity value compared to all films, 87%. However, in all PVA bio-composites, the addition of AG fiber showed increased crystallinity compared to pure PVA films. The lowest crystallinity was observed for PVA/UFG AG films (83%) and the highest for PVA/CMF AG (87%). The crystallinity value, however, is considerably higher than that reported by Abral et al., who found the highest crystallinity of films made from a PVA reinforced with bacterial cellulose nanofibers was only 66% (Abral et al. 2019).

The PVA/U2 AG peak at a value of 2θ 19.5° (2 0 0 field) also started to appear at higher concentrations of AG fiber. In PVA/U1 AG and PVA/U2 AG, the trend was not significant to increase crystallinity, which have the same crystallinity. This event can be described to the insignificant amount of cellulose micro-fiber in the PVA/U AG (wt./wt.) films. After that, crystallinity showed a slight increase with a 5% concentration in PVA/CMF AG films.

Thermogravimetry analysis (TGA) and derivative (DTG) assessment analysis

Figure 6 shows the thermal stability of PVA and PVA/CMF AG bio-composites through the TGA and DTG curves. The curves have the same patterns in the three weight loss regions in the temperature range of 75–410°C. The first area shows the evaporation of water vapor in the temperature range (80–165°C) with a weight loss range of 10–15 wt%. The second transition region (310–410°C) shows the decomposition of the structure of the PVA/MCF AG bio-composite films with a total weight loss of about 65–80 wt%.

The highest thermal stability of all PVA and PVA/CMF AG bio-composite film samples was PVA/U2 AG samples. These values, while not as high as that found for PVA/Uncaria gambir extract by boric acid (>369.5°C) (Rahmadiawan et al. 2022), are still sufficiently high to withstand microwaving. This phenomenon caused the addition of CMF after ultrasonication, causing the crystal structure to increase. This finding was validated by the measurement of the crystallinity index, as indicated in Table 1, and previous research. Because of the strong hydrogen connections formed between the PVA, cellulose, and matrix hydroxyl groups, this behavior suggests that adding CMF AG fiber can boost the heat stability of pure PVA (Khalili et al. 2022; Sun et al. 2019). The third region above 410°C shows residual charge formed from samples of PVA bio-composite films with a total weight loss above 96 wt % at 550°C. Another result that supports this discovery is that the PVA/U2 AG solution is extremely

Figure 7. Product sample of (a) PVA. (b) PVA CMF, (c) PVA UFG, (d) PVA U1, and (e) PVA U2.

well dispersed throughout the samples, promoting a strong connection between the cellulose molecules and the PVA matrix. This finding is in line with the recent findings of previous researchers (X. Han et al. 2023; S. S. Singh et al. 2022; Tiwari and Kumar Sarangi 2022; Tozluoğlu et al. 2017). The physical product of each sample is shown in Figure 7. According to the figure, the PVA U2 sample has a superior look and more uniformly stable surface stability than the other samples.

Differential Scanning Calorimetry (DSC), density, and thickness analysis

The thickness and density of each sample are explained in Figure 8. The thickness of the PVA sample is around 0.13 mm, smaller than the other samples. Meanwhile, the thickness of PVA/CMF AG was 0.22 mm, higher than the PVA/UFG, PVA/U1 AG, and PVA/U2 AG samples, with a thickness of around 0.19 mm. Meanwhile, the density of PVA is around 1.077 g/cm3, while the density of PVA/CMF AG is around 1.163 g/cm3, which is higher than the density because it is partially filled with cellulose. The density of the PVA/UFG, PVA/U1 AG, and PVA/U2 AG samples was higher, considering that the presence of cellulose microfiber in a tiny size does not cause large pores.

DSC thermograms of all samples are presented in Figure 9. Figure 9 shows the heating process of the PVA composite from 25°C to 300°C. For the PVA homopolymer, the DSC displays a glass transition (t_g) peak around 94.22°C with an enthalpy change $\Delta H \approx 204.20$ J/g. Another sharp endotherm melting transition (t_m) at 186.06°C with $\Delta H \approx 29.44$ J/g. The heat required to melt 100% PVA crystals is 138.6 J/g (Mathers et al. 2022). The presence of micro cellulose increased the value (t_g) of PVA to 113.57°C and the melting temperature to 187.74°C. The t_g temperature slowly shifts to a lower temperature, where the t_g of PVA/U2 AG is 106.83°C with a t_m of around 185.67°C. The enhancement of the glass transition can be attributed to the semicrystalline nature of the material. The t_g and t_m values are more consistent with previous

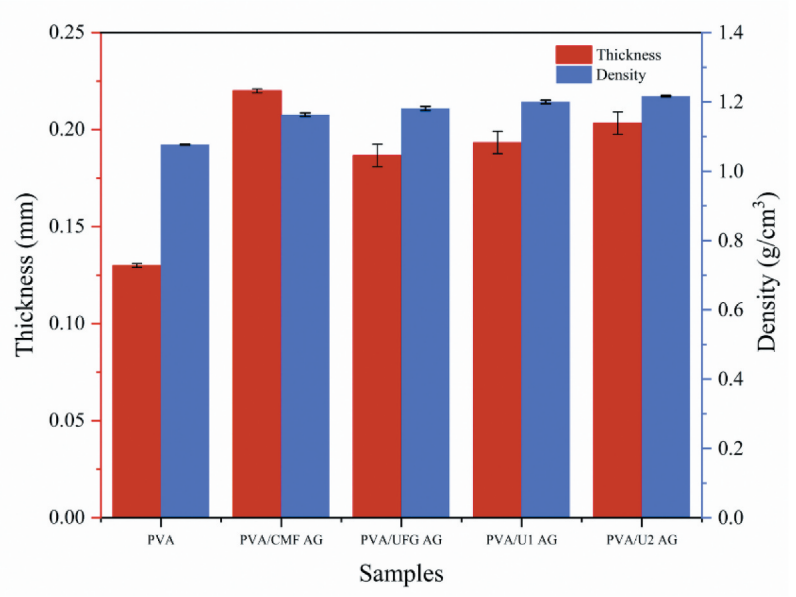

Figure 8. Thickness and density graphs of all samples.

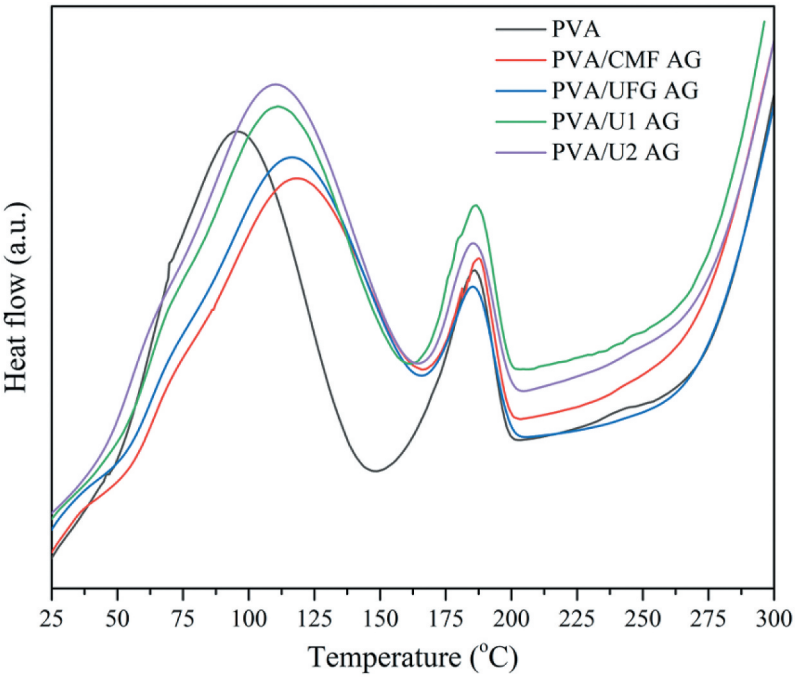

Figure 9. DSC thermogram PVA and PVA composites.

research (Okahisa et al. 2020). The enthalpy change from tg PVA/U2 AG is 225.43 J/g, and the enthalpy change from tm is 18.37 J/g.s.

Table 2. ANOVA summary.

Sample	Bursting strength (kg/cm^2)
S_1	16.08 ± 0.22
S_2	14.67 ± 0.16
S_3	12.96 ± 0.32
S_4	11.42 ± 0.26
S_5	10.27 ± 0.18
S_6	9.22 ± 0.24

Table 3. ANOVA output.

Source of Variation	SS	df	MS	F	P-value	F crit
Between Groups	418.862412	4	104.715	10.80004	0.000079	2.866081
Within Groups	193.917127	20	9.695856			
Total	612.779539	24				
Standard Error	0.95434569					
R^2	0.94600232					

ANOVA output

Table 2 displays the ANOVA output from the tensile strength test for each sample. Each sample was represented by five specimens: PVA, PVA/CMF, PVA/UFG, PVA/U1, and PVA/U2.

Table 2 summarizes the ANOVA analysis's number, average, and variance on the results of the tensile strength evaluation on the five types of samples. Based on the statistics, the pure PVA sample has a more excellent value than the PVA/CMF combination. According to the table, increasing the ultrasonication period increases the average tensile strength value. This summary of ANOVA statistics agrees well with the tensile strength result shown in Figure 4(a).

The ANOVA output is displayed in Table 3, where the square sum of inter-group ANOVA is 418.862412, and the sum of squares within groups is 193.917127. These two parameters represent the correlation of variation in the tensile strength population, with degrees of freedom of 4 and 20, respectively. Based on the results of Table 3, it is determined that there is a high correlation between the investigated factors and the response. The coefficient of determination value of 0.94600232 supports this event (Amroune et al. 2022). Although this investigation employed organic material, the coefficient of determination yielded a reasonably high value. The sample preparation and data retrieval of experimental findings performed five times enhances the data's confidence and reliability. This discovery is in line with previous researchers' coefficient of determination results (Choudhary, Sachdeva, and Kumar 2020; Nugroho et al. 2022).

The ANOVA output in this investigation fits well with the hypothesis that ultrafine grinding and ultrasonication time can enhance tensile strength with an F value of 10.80004. The p-value is lower than alpha 0.05, which is 0.000079. As a result, the hypothesis rejected Ho in this study's statistical analysis. This parameter is supported by the critical F value of 2.866081, much lower than the F value of 10.80004. This statistical evaluation is valid with a confidence level of 95% and a standard error of 0.95434569. Thus, the error of this statistical analysis is within 10%.

Conclusions

The production of PVA and PVA/CMF AG bio-composite films was successfully developed. CMF AG fiber has a diameter of 10–15 micrometers obtained from FESEM macroscopic and microscopic form of cellulose after chemical treatment (alkalization and bleaching) and ultrasonication method for 1 and

2 h. PVA/CMF bio-composite films were proven by analysis of mechanical properties, transparency, and thermal characterization. The effect of CMF in the PVA matrix has been investigated compressively. The tensile strength test on each sample revealed that the PVA/U2 bio-composite sample treated with ultrafine grinding and ultrasonication for 2 h had the most excellent tensile strength value compared to the other samples. The TGA and DTG analyses yielded similar results. This event demonstrates that the PVA/U2 sample has the most significant level of thermal stability. As a result, the PVA/U2 sample is an appropriate AG leaf-based microfiber sample that could be suggested for sustainable packaging applications. ANOVA output with an R2 value of 0.94600232 at a 95% confidence level supports the outcomes of this experiment. The p-value of 0.000079 and the F-value of 10.80004 for ultrafine grinding and ultrasonication time on AG leaf-based PVA bio-composite demonstrated strong significance, above the F-critical value of 2.866081. As a result, the F value fulfilled the statistical criteria for supporting the hypothesis (H1) and rejecting the null hypothesis (H0) within a 10% standard error.

Microfibers have been suggested as a potential material for packaging from an industrial perspective due to their unique properties. One of the main advantages of using microfibers in packaging is their high strength and durability. Microfibers are able to withstand high levels of stress and tension, making them suitable for packaging heavy or fragile items. This can help to prevent damage to the packaged items during transport and storage.

Another advantage of microfibers in packaging is their high barrier properties. They are able to prevent the penetration of gases, liquids, and bacteria, which can help to extend the shelf life of packaged products. Microfibers can also be used to create packaging that is resistant to punctures, tears, and other types of damage. Microfibers are also lightweight, which can help to reduce the overall weight and cost of packaging. This is important for shipping and transportation, as it can help to reduce fuel costs and lower the carbon footprint. Overall, microfibers are a versatile material for packaging, which can be tailored to the specific requirements of the packaged product, and their properties can be optimized for a specific application. Research in this area is ongoing to further develop their potential.

Highlights of this Investigation

- The production of PVA and PVA/CMF AG bio-composite films was successfully developed.
- Tensile testing revealed that the ultrafine grinding and ultrasonication treatment for 2 h (PVA/U2) increased tensile strength by 43% compared to the untreated PVA/CMF sample
- According to X-ray diffraction, the CMF bio-composite has the highest crystallinity index (87%).

Acknowledgements

This research work was funded by Institutional Fund Projects under grant no. (IFPIP-703-140-1443). The authors gratefully acknowledge technical and financial support provided by the Ministry of Education and King Abdulaziz University, DSR, Jeddah, Saudi Arabia. The authors would like to thank the Department of Agricultural Technology at Politeknik Pertanian Negeri Payakumbuh in West Sumatra and iLaB (Integrated Laboratory of Bioproducts), Research Center for Biomass and Bioproducts, National Research and Innovation Agency (BRIN) for their contributions to the success of this research.

Disclosure statement

No potential conflict of interest was reported by the authors.

Funding

This research work was funded by Institutional Fund Projects under grant no. (IFPIP-703-140-1443). The authors gratefully acknowledge technical and financial support provided by the Ministry of Education and King Abdulaziz University, DSR, Jeddah, Saudi Arabia.

ORCID

Edi Syafri http://orcid.org/0000-0002-5784-6694
Nasmi Herlina Sari http://orcid.org/0000-0002-6601-8487
Melbi Mahardika http://orcid.org/0000-0002-5468-3922
Anish Khan http://orcid.org/0000-0002-3806-5956

Author contribution

Melbi Mahardika, Edi Syafri, Jamaluddin, Nasmi Herlina Sari, Lisman Suryanegara designed the research and manuscript, data analysis while Ferriawan Yudhanto, Rahadian Zainul, Agus Nugroho, repeat the results and verify after that Rafles Sinaga, Anish Khan, Mohammad A. Wazzan write the final draft of the manuscript. Melbi Mahardika as corresponding Author.

Ethics approval and consent to participate

There is no need for any ethical approval in this study given here in this manuscript

References

Abdulkhani, A., Z. Echresh, and M. Allahdadi. 2020. Effect of nanofibers on the structure and properties of biocomposites. In *Fiber-reinforced nanocomposites: fundamentals and applications*, 321–57. Elsevier. doi:10.1016/B978-0-12-819904-6.00015-3.

Abolghasemi-Fakhri, L., B. Ghanbarzadeh, J. Dehghannya, F. Abbasi, and P. Adun. 2019. Styrene monomer migration from polystyrene based food packaging nanocomposite: Effect of clay and ZnO nanoparticles. *Food and Chemical Toxicology* 129:77–86. doi:10.1016/j.fct.2019.04.019.

Abral, H., J. Ariksa, M. Mahardika, D. Handayani, I. Aminah, N. Sandrawati, S. M. Sapuan, and R. A. Ilyas. 2020. Highly transparent and antimicrobial PVA based bionanocomposites reinforced by ginger nanofiber. *Polymer Testing* 81:106186. doi:10.1016/j.polymertesting.2019.106186.

Abral, H., M. Mahardika, D. Handayani, E. Sugiarti, A. Novi Muslimin, and A. N. Muslimin. 2019. Characterization of disintegrated bacterial cellulose nanofibers/PVA bionanocomposites prepared via ultrasonication. *International Journal of Biological Macromolecules* 135:591–99. doi:10.1016/j.ijbiomac.2019.05.178.

Akoueson, F., I. Paul-Pont, K. Tallec, A. Huvet, P. Doyen, A. Dehaut, and G. Duflos. 2023. Additives in polypropylene and polylactic acid food packaging: Chemical analysis and bioassays provide complementary tools for risk assessment. *The Science of the Total Environment* 857:159318. doi:10.1016/j.scitotenv.2022.159318.

Allafchian, A. R., S. Kalani, P. Golkar, H. Mohammadi, and S. Amir Hossein Jalali. 2020. A comprehensive study on plantago ovata/PVA biocompatible nanofibers: Fabrication, characterization, and biological assessment. *Journal of Applied Polymer Science* 137 (47):49560. doi:10.1002/app.49560.

Amroune, S., A. Belaadi, R. Dalmis, Y. Seki, A. Makhlouf, and H. Satha. 2022. Quantitatively investigating the effects of fiber parameters on tensile and flexural response of flax/epoxy biocomposites. *Journal of Natural Fibers* 19 (6):2366–81. doi:10.1080/15440478.2020.1817831.

Anwer, M. A. S., H. E. Naguib, A. Celzard, and V. Fierro. 2015. Comparison of the thermal, dynamic mechanical and morphological properties of PLA-Lignin & PLA-Tannin particulate green composites. *Composites Part B: Engineering* 82:92–99. doi:10.1016/j.compositesb.2015.08.028.

ASTM. 2006. *Standard test method for haze and luminous transmittance of transparent plastics*. American Society for Testing and Materials ASTM D1003.

ASTM. 2012. *Standard test method for tensile properties of thin plastic sheeting*. American Society for Testing and Materials D638-V.

Azammi, A. M. N., R. A. Ilyas, S. M. Sapuan, R. Ibrahim, M. S. N. Atikah, M. Asrofi, and A. Atiqah. 2020. Characterization studies of biopolymeric matrix and cellulose fibres based composites related to functionalized fibre-matrix interface. In *Interfaces in particle and fibre reinforced composites*, 29–93. Elsevier. doi:10.1016/B978-0-08-102665-6.00003-0.

Candan, Z., D. J. Gardner, and S. M. Shaler. 2016. Dynamic Mechanical Thermal Analysis (DMTA) of cellulose Nanofibril/Nanoclay/PMDI nanocomposites. *Composites Part B: Engineering* 90:126–32. doi:10.1016/j.compositesb.2015.12.016.

Candan, Z., A. Tozluoglu, O. Gonultas, M. Yildirim, H. Fidan, M. Hakki Alma, and T. Salan. 2022. Nanocellulose: Sustainable biomaterial for developing novel adhesives and composites. In *Industrial applications of nanocellulose and its nanocomposites*, 49–137. Elsevier. doi:10.1016/B978-0-323-89909-3.00015-8.

Cano, A. I., M. Cháfer, A. Chiralt, and C. González-Martínez. 2015. Physical and microstructural properties of biodegradable films based on pea starch and PVA. *Journal of Food Engineering* 167:59–64. doi:10.1016/j.jfoodeng.2015.06.003.

Cazón, P., M. Vázquez, and G. Velazquez. 2018a. Cellulose-glycerol-polyvinyl alcohol composite films for food packaging: Evaluation of water adsorption, mechanical properties, light-barrier properties and transparency. *Carbohydrate Polymers* 195:432–43. doi:10.1016/j.carbpol.2018.04.120.

Cazón, P., M. Vázquez, and G. Velazquez. 2018b. Novel composite films based on cellulose reinforced with chitosan and polyvinyl alcohol: Effect on mechanical properties and water vapour permeability. *Polymer Testing* 69:536–44. doi:10.1016/j.polymertesting.2018.06.016.

Chen, J., M. Zheng, K. Bing Tan, J. Lin, M. Chen, and Y. Zhu. 2022. Polyvinyl alcohol/xanthan gum composite film with excellent food packaging, storage and biodegradation capability as potential environmentally-friendly alternative to commercial plastic bag. *International Journal of Biological Macromolecules* 212:402–11. doi:10.1016/j.ijbiomac.2022.05.119.

Choudhary, S., A. Sachdeva, and P. Kumar. 2020. Investigation of the stability of MgO nanofluid and its effect on the thermal performance of flat plate solar collector. *Renewable Energy* 147:1801–14. doi:10.1016/j.renene.2019.09.126.

Dara, P. K., G. K. Sivaraman, K. Deekonda, A. Rangasamy, S. Mathew, C. N. Ravishankar, S. Mathew, and R. Cn. 2021. Biomodulation of poly (vinyl alcohol)/starch polymers into composite-based hybridised films: physico-chemical, structural and biocompatibility characterization. *Journal of Polymer Research* 28 (7):265. doi:10.1007/s10965-021-02578-y.

da Silva, D. J., M. M. de Oliveira, S. Hui Wang, D. J. Carastan, and D. S. Rosa. 2022. Designing antimicrobial polypropylene films with grape pomace extract for food packaging. *Food Packaging and Shelf Life* 34:100929. doi:10.1016/j.fpsl.2022.100929.

Ding, Z., Y. Tang, and P. Zhu. 2022. Reduced graphene oxide/cellulose nanocrystal composite films with high specific capacitance and tensile strength. *International Journal of Biological Macromolecules* 200:574–82. doi:10.1016/j.ijbiomac.2022.01.130.

Doustdar, F., A. Olad, and M. Ghorbani. 2022. Effect of glutaraldehyde and calcium chloride as different crosslinking agents on the characteristics of chitosan/cellulose nanocrystals scaffold. *International Journal of Biological Macromolecules* 208:912–24. doi:10.1016/j.ijbiomac.2022.03.193.

Feiya, F., L. Lingyan, L. Liu, J. Cai, Y. Zhang, J. Zhou, and L. Zhang. 2015. Construction of cellulose based ZnO nanocomposite films with antibacterial properties through one-step coagulation. *ACS Applied Materials & Interfaces* 7 (4):2597–606. doi:10.1021/am507639b.

Haider, T. P., C. Völker, J. Kramm, K. Landfester, and F. R. Wurm. 2019. Plastics of the future? The impact of biodegradable polymers on the environment and on society. *Angewandte Chemie International Edition* 58 (1):50–62. doi:10.1002/anie.201805766.

Han, X., L. Ding, Z. Tian, Y. Song, R. Xiong, C. Zhang, J. Han, and S. Jiang. 2023. Potential new material for optical fiber: Preparation and characterization of transparent fiber based on natural cellulosic fiber and epoxy. *International Journal of Biological Macromolecules* 224:1236–43. doi:10.1016/j.ijbiomac.2022.10.209.

Han, Y., Y. Jiang, and H. Jinlian. 2020. Tea-polyphenol treated skin collagen owns coalesced adaptive-hydration, tensile strength and shape-memory property. *International Journal of Biological Macromolecules* 158:1–8. doi:10.1016/j.ijbiomac.2020.04.002.

Huang, B., H. He, H. Liu, W. Wu, Y. Ma, and Z. Zhao. 2019. Mechanically strong, heat-resistant, water-induced shape memory poly (vinyl alcohol)/regenerated cellulose biocomposites via a facile co-precipitation method. *Biomacromolecules* 20 (10):3969–79. doi:10.1021/acs.biomac.9b01021.

Hu, D., and L. Wang. 2016. Physical and antibacterial properties of polyvinyl alcohol films reinforced with quaternized cellulose. *Journal of Applied Polymer Science* 133:25. doi:10.1002/app.43552.

Jahan, Z., M. Bilal Khan Niazi, and Ø. Weiby Gregersen. 2018. Mechanical, thermal and swelling properties of cellulose nanocrystals/PVA nanocomposites membranes. *Journal of Industrial and Engineering Chemistry* 57:113–24. doi:10.1016/j.jiec.2017.08.014.

Jain, N., V. Kumar Singh, and S. Chauhan. 2017. A review on mechanical and water absorption properties of polyvinyl alcohol based composites/films. *Journal of the Mechanical Behavior of Materials* 26 (5–6):213–22. doi:10.1515/jmbm-2017-0027.

Joshi, S., and S. Patel. 2022. Review on mechanical and thermal properties of pineapple leaf fiber (PALF) reinforced composite. *Journal of Natural Fibers* 19 (15):10157–78. doi:10.1080/15440478.2021.1993487.

Kalambettu, A., A. Damodaran, S. Dharmalingam, and M. Tindivanam Vallam. 2015. Evaluation of biodegradation of pineapple leaf fiber reinforced PVA composites. *Journal of Natural Fibers* 12 (1):39–51. doi:10.1080/15440478.2014.880104.

Kashyap, P. K., S. Chauhan, Y. Singh Negi, N. Kumar Goel, and S. Rattan. 2022. Biocompatible carboxymethyl chitosan-modified glass ionomer cement with enhanced mechanical and anti-bacterial properties. *International Journal of Biological Macromolecules* 223:1506–20. doi:10.1016/j.ijbiomac.2022.11.028.

Khalili, H., M. Hamid Salim, S.E. Jabor Tlemcani, R. Makhlouf, F.Z. Semlali Aouragh Hassani, H. Ablouh, Z. Kassab, and M. El Achaby. 2022. Bio-nanocomposite films based on cellulose nanocrystals filled polyvinyl alcohol/alginate polymer blend. *Journal of Fibers and Polymer Composites* 1 (2):77–96. doi:10.55043/jfpc.v1i2.56.

Kumar, R., K. Kumar, and S. Bhowmik. 2018. Assessment and response of treated cocos nucifera reinforced toughened epoxy composite towards fracture and viscoelastic properties. *Journal of Polymers and the Environment* 26:2522–35. doi:10.1007/s10924-017-1150-y.

Lisdayana, N., F. Fahma, T. Candra Sunarti, and E. Savitri Iriani. 2020. Thermoplastic starch–PVA nanocomposite films reinforced with nanocellulose from oil palm empty fruit bunches (OPEFBs): Effect of starch type. *Journal of Natural Fibers* 17 (7):1069–80. doi:10.1080/15440478.2018.1558142.

Li, Y., M. Yao, C. Liang, H. Zhao, Y. Liu, and Y. Zong. 2022. Hemicellulose and nano/microfibrils improving the pliability and hydrophobic properties of cellulose film by interstitial filling and forming micro/nanostructure. *Polymers* 14 (7):1297. doi:10.3390/polym14071297.

Mahardika, M., H. Abral, A. Kasim, S. Arief, F. Hafizulhaq, and M. Asrofi. 2019. Properties of cellulose nanofiber/bengkoang starch bionanocomposites: effect of fiber loading. *LWT* 108554:108554. doi:10.1016/j.lwt.2019.108554.

Mathers, A., M. Pechar, F. Hassouna, and M. Fulem. 2022. API solubility in semi-crystalline polymer: Kinetic and thermodynamic phase behavior of PVA-based solid dispersions. *International Journal of Pharmaceutics* 623:121855. doi:10.1016/j.ijpharm.2022.121855.

Mohammadi, S., and A. Babaei. 2022. Poly (vinyl alcohol)/chitosan/polyethylene glycol-assembled graphene oxide bio-nanocomposites as a prosperous candidate for biomedical applications and drug/food packaging industry. *International Journal of Biological Macromolecules* 201:528–38. doi:10.1016/j.ijbiomac.2022.01.086.

Moradi, E., M. Hashemi Moosavi, S. Marzieh Hosseini, L. Mirmoghtadaie, M. Moslehishad, M. Reza Khani, N. Jannatyha, and S. Shojaee-Aliabadi. 2020. Prolonging shelf life of chicken breast fillets by using plasma-improved chitosan/low density polyethylene bilayer film containing summer savory essential oil. *International Journal of Biological Macromolecules* 156:321–28. doi:10.1016/j.ijbiomac.2020.03.226.

Niazi, M. B. K., Z. Jahan, S. Sofie Berg, and Ø. Weiby Gregersen. 2017. Mechanical, thermal and swelling properties of phosphorylated nanocellulose fibrils/PVA nanocomposite membranes. *Carbohydrate Polymers* 177:258–68. doi:10.1016/j.carbpol.2017.08.125.

Nugroho, A., Z. Bo, R. Mamat, W. H. Azmi, G. Najafi, and F. Khoirunnisa. 2021. Extensive examination of sonication duration impact on stability of Al2O3-polyol ester nanolubricant. *International Communications in Heat and Mass Transfer* 126:105418. doi:10.1016/j.icheatmasstransfer.2021.105418.

Nugroho, A., R. Mamat, Z. Bo, W. Azmi Wan Hamzah, M. Fairusham Ghazali, and T. Yusaf. 2022. "Surface modification for dispersion stability of novel FAl2O3-POE nanolubricant using functional SiO2." In *Proceedings of the 2nd Energy Security and Chemical Engineering Congress: Selected Articles from ESChE 2021*, Malaysia, 179–92. Springer. doi:10.1007/978-981-19-4425-3_17.

Nurazzi, N. M., M. R. M. Asyraf, M. Rayung, M. N. F. Norrrahim, S. S. Shazleen, M. S. A. Rani, A. R. Shafi, H. A. Aisyah, M. H. M. Radzi, and F. A. Sabaruddin. 2021. Thermogravimetric analysis properties of cellulosic natural fiber polymer composites: A review on influence of chemical treatments. *Polymers* 13 (16):2710. doi:10.3390/polym13162710.

Okahisa, Y., K. Matsuoka, K. Yamada, and I. Wataoka. 2020. Comparison of polyvinyl alcohol films reinforced with cellulose nanofibers derived from oil palm by impregnating and casting methods. *Carbohydrate Polymers* 250:116907. doi:10.1016/j.carbpol.2020.116907.

Pilevar, Z., A. Bahrami, S. Beikzadeh, H. Hosseini, and S. Mahdi Jafari. 2019. Migration of styrene monomer from polystyrene packaging materials into foods: Characterization and safety evaluation. *Trends in Food Science & Technology* 91:248–61. doi:10.1016/j.tifs.2019.07.020.

Poyraz, B., A. Tozluoğlu, Z. Candan, and A. Demir. 2017. Matrix impact on the mechanical, thermal and electrical properties of microfluidized nanofibrillated cellulose composites. *Journal of Polymer Engineering* 37 (9):921–31. doi:10.1515/polyeng-2017-0022.

Poyraz, B., A. Tozluoğlu, Z. Candan, A. Demir, M. Yavuz, Ü. Büyuksarı, H. İbrahim Ünal, H. Fidan, and R. Cem Saka. 2018. TEMPO-Treated CNf composites: pulp and matrix effect. *Fibers and Polymers* 19 (1):195–204. doi:10.1007/s12221-018-7673-y.

Rahmadiawan, D., H. Abral, R. Muhammad Railis, I. Chayri Iby, M. Mahardika, D. Handayani, K. Dwi Natrana, D. Juliadmi, and F. Akbar. 2022. The enhanced moisture absorption and tensile strength of PVA/Uncaria gambir extract by boric acid as a highly moisture-resistant, anti-UV, and strong film for food packaging applications. *Journal of Composites Science* 6 (11):337. doi:10.3390/jcs6110337.

Sarwar, M. S., M. Bilal Khan Niazi, Z. Jahan, T. Ahmad, and A. Hussain. 2018. Preparation and characterization of PVA/nanocellulose/Ag nanocomposite films for antimicrobial food packaging. *Carbohydrate Polymers* 184:453–64. doi:10.1016/j.carbpol.2017.12.068.

Singh, S., K. K. Gaikwad, and Y. Suk Lee. 2018. Antimicrobial and antioxidant properties of polyvinyl alcohol bio composite films containing seaweed extracted cellulose nano-crystal and basil leaves extract. *International Journal of Biological Macromolecules* 107:1879–87. doi:10.1016/j.ijbiomac.2017.10.057.

Singh, S. K., S. Khan, R. Kumar Mishra, and J. Karloopia. 2021. Fabrication and evaluation of mechanical properties of polymer matrix composite using nano fibers as a reinforcement. *Materials Today: Proceedings* 46:1376–83. doi:10.1016/j.matpr.2021.02.488.

Singh, S. S., A. Zaitoon, S. Sharma, A. Manickavasagan, and L.T. Lim. 2022. Enhanced hydrophobic paper-sheet derived from miscanthus× giganteus cellulose fibers coated with esterified lignin and cellulose acetate blend. *International Journal of Biological Macromolecules* 223:1243–56. doi:10.1016/j.ijbiomac.2022.11.066.

Solikhin, A., Y. Sudo Hadi, M. Yusram Massijaya, S. Nikmatin, S. Suzuki, Y. Kojima, and H. Kobori. 2018. Properties of poly (vinyl alcohol)/chitosan nanocomposite films reinforced with oil palm empty fruit bunch amorphous lignocellulose nanofibers. *Journal of Polymers and the Environment* 26:3316–33. doi:10.1007/s10924-018-1215-6.

Sultana, T., S. Sultana, H. Parvin Nur, and M. Wahab Khan. 2020. Studies on mechanical, thermal and morphological properties of betel nut husk nano cellulose reinforced biodegradable polymer composites. *Journal of Composites Science* 4 (3):83. doi:10.3390/jcs4030083.

Sun, J., Y. Pang, Y. Yang, J. Zhao, R. Xia, Y. Li, Y. Liu, and H. Guo. 2019. Improvement of rice Husk/HDPE biocomposites interfacial properties by silane coupling agent and compatibilizer complementary modification. *Polymers* 11 (12):1928. doi:10.3390/polym11121928.

Syafri, E., N. Herlina Sari, M. Mahardika, P. Amanda, R. Ahmad Ilyas, and R. A. Ilyas. 2021. Isolation and characterization of cellulose nanofibers from agave gigantea by chemical-mechanical treatment. *International Journal of Biological Macromolecules* 200:25–33. doi:10.1016/j.ijbiomac.2021.12.111.

Syafri, E., S. Melly, I. Anas, A. Defrian, S. Umar, and M. Mahardika. 2021. Extraction and characterization of agave gigantea fibers with alkali treatment as reinforcement for composites. *Journal of Natural Fibers* 19:1–10. doi:10.1080/15440478.2021.1964124.

Taghavi, N., I. Abeykoon Udugama, W.Q. Zhuang, and S. Baroutian. 2021. Challenges in biodegradation of non-degradable thermoplastic waste: From environmental impact to operational readiness. *Biotechnology Advances* 49:107731. doi:10.1016/j.biotechadv.2021.107731.

Taspika, M., R. Dwi Desiati, M. Mahardika, E. Sugiarti, and H. Abral. 2020. Influence of TiO2/Ag particles on the properties of chitosan film. *Advances in Natural Sciences: Nanoscience and Nanotechnology* 11 (1):15017. doi:10.1088/2043-6254/ab790e.

Tiwari, Y. M., and S. Kumar Sarangi. 2022. Characterization of raw and alkali treated cellulosic grewia flavescens natural fiber. *International Journal of Biological Macromolecules* 209:1933–42. doi:10.1016/j.ijbiomac.2022.04.169.

Tozluoglu, A., S. Ates, E. Durmaz, S. Sertkaya, R. Arslan, O. Ozcelik, and Z. Candan. 2022. Nanocellulose in paper and board coating. In *Emerging nanomaterials: Opportunities and challenges in forestry sectors*, 197–298. Springer. doi:10.1007/978-3-031-17378-3.

Tozluoğlu, A., B. Poyraz, Z. Candan, M. Yavuz, and R. Arslan. 2017. Biofilms from micro/nanocellulose of modified kraft pulp. *Bulletin of Materials Science* 40 (4):699–710. doi:10.1007/s12034-017-1416-y.

Wang, Q., H. Du, F. Zhang, Y. Zhang, M. Wu, G. Yu, C. Liu, B. Li, and H. Peng. 2018. Flexible cellulose nanopaper with high wet tensile strength, high toughness and tunable ultraviolet blocking ability fabricated from tobacco stalk via a sustainable method. *Journal of Materials Chemistry A* 6 (27):13021–30. doi:10.1039/C8TA01986J.

Wang, C., N. Wang, S. Liu, L.P. Choo-Simth, H. Zhang, and Z. Zhi. 2020. Investigation of microfibril angle of flax fibers using X-Ray diffraction and scanning electron microscopy. *Journal of Natural Fibers* 17 (7):1001–10. doi:10.1080/15440478.2018.1546639.

Wang, H., T. Xue, S. Wang, X. Jia, S. Cao, B. Niu, R. Guo, and H. Yan. 2022. Preparation, characterization and food packaging application of nano ZnO@ xylan/quaternized xylan/polyvinyl alcohol composite films. *International Journal of Biological Macromolecules* 215:635–45. doi:10.1016/j.ijbiomac.2022.06.157.

Wu, J., D. Wang, F. Meng, J. Li, C. Huo, X. Du, and S. Xu. 2022. Polyvinyl alcohol based bio-composite films reinforced by liquefaction products and cellulose nanofibrils from coconut coir. *Journal of Applied Polymer Science* 139 (12):51821. doi:10.1002/app.51821.

Yuan, H., G. Liu, Y. Chen, Y. Zhiwei, W. Jin, and G. Zhang. 2023. A versatile tag for simple preparation of cutinase towards enhanced biodegradation of polyethylene terephthalate. *International Journal of Biological Macromolecules* 225:149–61. doi:10.1016/j.ijbiomac.2022.11.126.

Yun, D., Y. He, H. Zhu, Y. Hui, C. Li, D. Chen, and J. Liu. 2022. Smart packaging films based on locust bean gum, polyvinyl alcohol, the crude extract of loropetalum chinense var. Rubrum petals and its purified fractions. *International Journal of Biological Macromolecules* 205:141–53. doi:10.1016/j.ijbiomac.2022.02.068.

Zhai, X., S. Zhou, R. Zhang, W. Wang, and H. Hou. 2022. Antimicrobial Starch/Poly (butylene adipate-co-terephthalate) nanocomposite films loaded with a combination of silver and zinc oxide nanoparticles for food packaging. *International Journal of Biological Macromolecules* 206:298–305. doi:10.1016/j.ijbiomac.2022.02.158.